Molecular Weight Effects in the Third-Harmonic Generation Spectroscopy of Thin Films of the Conjugated Polymer MEH-PPV

Ayi Bahtiar,[†] Kaloian Koynov, Taek Ahn,[‡] and Christoph Bubeck*

Max Planck Institute for Polymer Research, Ackermannweg 10, D-55128 Mainz, Germany

Received: August 31, 2007; In Final Form: January 8, 2008

Thin spin-cast films of poly[2-methoxy-5-(2′-ethyl-hexyloxy)-1,4-phenylenevinylene] (MEH-PPV) were prepared from samples whose weight-average molecular weight (M_w) was varied in the range of 10−1600 kg/mol. We have characterized the films by means of transmission and reflection ultraviolet−visible−near-infrared (UV−vis−NIR) spectroscopy to derive the linear optical constants, and third-harmonic generation spectroscopy with variable laser wavelengths to get the modulus and phase angles of the complex third-order nonlinear optical susceptibility $\chi^{(3)}$. Increasing molecular weight yields films with significantly larger $\chi^{(3)}$ values, absorption coefficients, and refractive indices. The $\chi^{(3)}$ values of films from the largest and lowest M_w differ by a factor of 4, which is caused by chain orientation effects, local field effects, and changes of the effective conjugation length.

Introduction

Poly(1,4-phenylenevinylene) (PPV) and its derivatives find continuing scientific interest because of their favorable photophysical properties for optoelectronic devices[1−3] such as organic light emitting diodes (OLEDs),[4,5] solar cells,[6] and plastic lasers,[7] and for third-order nonlinear optics.[8−29] The PPV derivative poly[2-methoxy-5-(2′-ethyl-hexyloxy)-1,4-phenylenevinylene] (MEH-PPV, see Scheme 1 for its chemical structure) is particularly suitable for the preparation of thin films, as it is fully soluble in common organic solvents and can be processed by spin-coating.[22−44] The synthesis of MEH-PPV is performed using two alternate chemical routes: The so-called Gilch route usually yields high molecular weight PPVs with a weight average molecular weight (M_w) on the order of 10^5−10^6 g/mol.[45−47] The Horner route, on the other hand, is most suitable for highly pure MEH-PPV with $M_w = (2-4) \times 10^4$ g/mol.[30−32] Recently, we have shown that Horner route MEH-PPVs can be processed to optical slab waveguides with propagation losses of 1 dB/cm or less,[24−27,35] i.e., to values suitable for integrated optical circuits.[48] Furthermore, MEH-PPV already satisfies the figures of merit for ultrafast all-optical switching applications[49,50] in a spectral window around 1100 nm.[25,29]

It is well-known that the chain length, i.e., the molecular weight, has major influence on the linear and nonlinear optical properties of one-dimensional conjugated π-electron systems. Short chains such as conjugated oligomers show a significant increase in the wavelength of the maximum of the main absorption band (λ_{max}) and the second hyperpolarizability (γ) per repeat unit, which usually follow power law dependencies of the chain length in a regime up to approximately 2 nm.[10,11,18,51] For chain lengths larger than typically 2 nm, so-called saturation effects are observed, which means that λ_{max} and γ per repeat unit converge to finite values that are sensitively dependent on the chemical structure and conformation of the polymer.[52−60] However, it was noted recently that the two-photon absorption coefficient of thin films of a polydiacetylene can still increase with M_w, even if M_w is significantly larger than the saturation limit of γ per repeat unit.[61] This behavior was attributed to chain ordering effects in thin films which can have strong impact on the third-order nonlinear optical properties of thin films of conjugated polymers.[62,63]

SCHEME 1: Chemical Structure of Poly[2-methoxy-5-(2′-ethyl-hexyloxy)-1,4-phenylene-vinylene] (MEH-PPV)

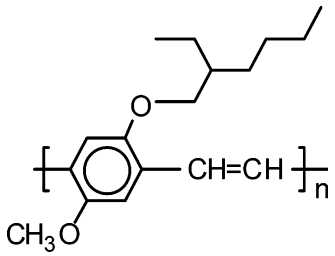

Thin polymer films usually exhibit strong uniaxial anisotropy due to the preferred alignment of polymer chains parallel to the film plane.[34,35,42−44,64−67] This effect becomes particularly pronounced for rigid polymer chains. As the electric polarizability and the transition dipole moment of the conjugated π-electron system are mainly parallel to the chain direction, the anisotropic orientation of chain segments is strongly correlated with significant birefringence of the films, i.e., the in-plane refractive index at transverse electric polarization (n_{TE}) is much larger than the out-of-plane index at transverse magnetic polarization (n_{TM}). Numerous studies report the birefringence of MEH-PPV films.[34,35,42−44,64,65] Aggregate formation can occur in solutions already and in thin films of high molecular weight MEH-PPVs, which might cause chain orientation effects.[28,36−38] Recently, we reported that the birefringence of thin MEH-PPV films increases strongly with M_w,[34,35] ranging from nearly isotropic to almost two-dimensional chain orientation parallel to the layer plane. Consequently, the linear optical constants of the films, i.e., their absorption, refractive index and birefringence also increase significantly with M_w.[34,35] Nevertheless, the

* Corresponding author. E-mail: bubeck@mpip-mainz.mpg.de.
[†] Present address: Department of Physics, University of Padjadjaran Bandung, Jl. Jatinangor km. 21 Sumedang, 45363, Indonesia.
[‡] Present address: Information and Electronics Polymer Research Center, Korea Research Institute of Chemical Technology, P.O. Box 107, Yuseong, Daejeon 305-600, Korea.

10.1021/jp077006w CCC: $40.75
Published on Web 03/01/2008

TABLE 1: Molecular Weights (M_w: Weight Average, M_n: Number Average) of MEH-PPVs from Different Synthetic Routes and Sources: American Dye Source (ADS), Max Planck Institute for Polymer Research (MPI-P), and Prof. H.-H. Hörhold (University of Jena)

polymer	route	M_w [kg/mol]	M_n [kg/mol]	M_w/M_n	source
1	Gilch	9.3	4.8	1.94	ADS, Canada
2	Horner	13	6.4	2.03	MPI-P
3	Horner	25	9.1	2.75	Univ. Jena
4	Horner	40.3	14.1	2.86	Univ. Jena
5	Gilch	265	87.1	3.04	ADS, Canada
6	Gilch	276	105	2.63	MPI−P
7	Gilch	420	108	3.89	ADS, Canada
8	Gilch	1600	130	12.3	Covion, Germany

underlying mechanisms causing the preferred in-plain chain orientation are still not completely understood.

The aim of this paper is a comprehensive study of the influence of M_w on the third-order nonlinear optical susceptibility $\chi^{(3)}$ of thin films of MEH-PPV. We used third-harmonic generation (THG) spectroscopy to measure $\chi^{(3)}$ of thin spin-cast films, prepared from MEH-PPVs that had M_w from 10 to 1600 kg/mol. THG is important for analytical purposes as THG probes the purely electronic nonlinear response of the sample with high sensitivity, in contrast to other methods based on measurements of the intensity dependent refractive index, which may suffer from thermally induced effects. THG spectroscopy is a versatile method to resolve $\chi^{(3)}(-3\omega;\omega,\omega,\omega)$, where the frequency ω is related to the laser wavelength λ_L. The so-called three-photon resonance occurs if the laser wavelength λ_L is close to $3\lambda_{max}$.[10,18] There, $\chi^{(3)}$ approaches the maximum value $\chi^{(3)}_{max}$. We have studied the resonance behavior of $\chi^{(3)}(-3\omega;\omega,\omega,\omega)$ using tunable laser wavelengths in the near-infrared. Our results show that the $\chi^{(3)}_{max}$ of the MEH-PPV films can increase as much as a factor 4 with the increase of M_w. We discuss the origin of this effect by considering local field effects,[68] orientation phenomena, and influences of the effective conjugation lengths in the polymer films.

Experimental Section

Materials. We investigated eight different MEH-PPV samples **1**−**8** (listed in Table 1) with a weight average molecular weight M_w in the range of 10−1600 kg/mol. We used polymers from different sources and synthetic routes. MEH-PPVs **2**−**4** were synthesized via the polycondensation route using carbonylolefination as the step growth polymerization process, the so-called Horner route.[30−32] The synthesis of **6** was performed via the Gilch dehydrohalogenation as described recently.[69] MEH-PPVs **1**, **5**, **7**, and **8** were also synthesized via the Gilch route and obtained different sources as listed in Table 1. Molecular weights were measured by gel permeation chromatography (GPC) using polystyrene standards and tetrahydrofuran (THF) as eluent.

Thin Film Preparation. Thin films on fused silica substrates were deposited by spin coating from freshly prepared and filtered (0.5−1 μm syringe filters) toluene solutions at ambient temperature under a laminar flow hood to minimize dust particles, as described in detail recently.[27,35] We varied solution concentration and spinning speed to achieve a typical film thickness d in the range 50−70 nm. Subsequently, the samples were placed in a vacuum oven at elevated temperatures ($T \approx 50$ °C) for at least 6 h to remove residual solvent.

Thin Film Characterization. The film thickness d was measured with a Tencor Model P10 step-profiler. We have measured d for each sample at several places (typically eight) in the region where the optical experiments were performed and used the average value of these measurements. In all spectroscopic studies described below, we used films with typical thicknesses on the order of 50−70 nm.

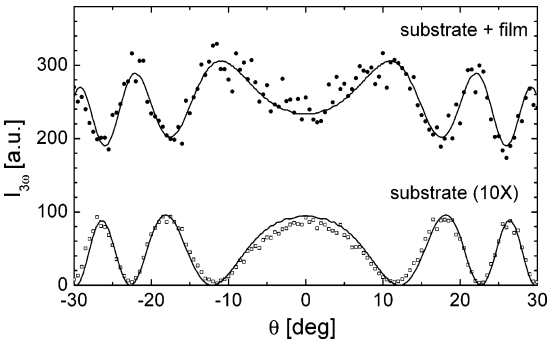

Figure 1. Angular dependence of the third-harmonic intensity for a 70 nm thick film of polymer **2** on the front side of a 1 mm thick fused silica substrate (full symbols), and the substrate alone after wiping off the polymer film (open symbols) at a laser wavelength $\lambda_L = 1470$ nm. The solid lines show the theoretical fits.

The dispersions of the absorption coefficient $\alpha(\lambda)$ and the refractive index $n(\lambda)$ of each film were determined from transmission and reflection spectra measured with a ultraviolet−visible−near-infrared (UV−vis−NIR) spectrometer (Perkin-Elmer Model Lambda 900) following the same measurement principles as described in our earlier work.[18,27,35] We used polarized light with the electrical field vector parallel to the film plane. Therefore, the in-plane components of $\alpha(\lambda)$ and refractive index n_{TE} were evaluated. We obtain the intrinsic absorption coefficient $\alpha(\lambda)$ by subtracting the reflection losses at the film/air and film/substrate interfaces from the measured transmission spectra.[18,27,35]

THG Spectroscopy. THG spectra of thin films of MEH-PPV films were measured by means of the Maker fringe technique[18,70,71] using the experimental setup described recently.[57,72] In short, we used an optical parametric generator (OPG: EKSPLA, model PG 501), which produces laser pulses with a duration of 20 ps, a repetition rate 10 Hz, and a wavelength tuning range between 680 and 2000 nm. This laser beam was polarized with the electric field parallel to the film plane and focused on the sample, which was placed in an evacuated chamber and mounted on a rotation stage. The intensity of the THG signal generated from the sample was measured as a function of the incidence angle θ. Typical Maker fringe patterns of a thin film on substrate and a substrate alone are shown in Figure 1 for comparison. We used the same evaluation procedure as described in our earlier work[18,57,71,72] to fit the experimentally measured Maker fringe patterns. Our evaluation procedure involves data of the sample, which we measured separately: thickness, refractive index, and absorption coefficients at the fundamental and harmonic laser wavelengths (λ_L, $\lambda_L/3$) for film and quartz substrate, respectively. We apply a matrix formalism to calculate the electric fields of all forward and backward reflected waves in the layer system, including the so-called free and bound harmonic waves and their reflections at the interfaces, as described in detail earlier.[71] This way we obtain the theoretical fit of the measured Maker fringes. We used two fitting parameters only: the modulus $|\chi^{(3)}|$ and the phase angle φ of the macroscopic, complex third-order susceptibility

$$\chi^{(3)}(-3\omega,\omega,\omega,\omega) = |\chi^{(3)}| \exp(i\varphi) \qquad (1)$$

of the films. The values of the orientation average of $\langle|\chi^{(3)}(-3\omega;\omega,\omega,\omega)|\rangle$ with the electric field vector parallel to the

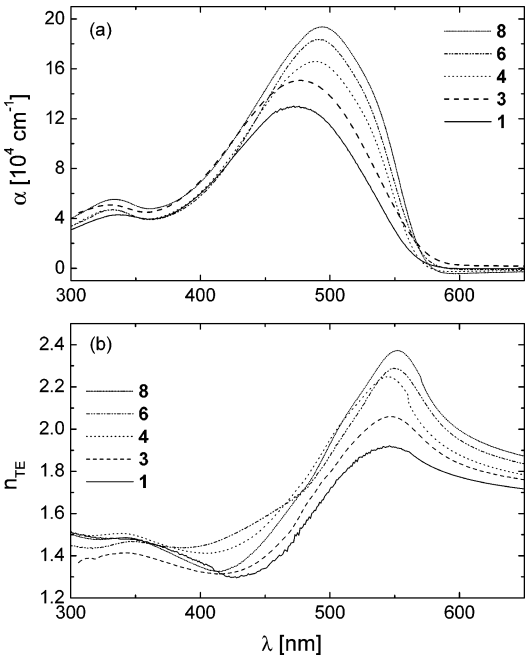

Figure 2. Spectra of the intrinsic in-plane absorption coefficient α (a) and the in-plane refractive index n_{TE} (b) of thin films of MEH-PPVs **1**, **3**, **4**, **6**, and **8**.

layer plane were determined with respect to the reference value of the fused silica substrate using $|\chi^{(3)}_{quartz}| = 3.11 \times 10^{-14}$ esu for all laser wavelengths.[70]

Results and Discussion

Linear Optical Spectroscopy. As mentioned above, the evaluation of the third-order susceptibility $\chi^{(3)}$ needs a detailed knowledge of the linear optical constants of the films, i.e., their refractive indices and absorption coefficients. Therefore, we measured the values of these constants for all films between 300 and 1700 nm. Selected spectra of $\alpha(\lambda)$ and $n_{TE}(\lambda)$ for polymers **1**, **3**, **4**, **6**, and **8** are shown in Figure 2, panels a and b, respectively. The absorption coefficients α_{max} and the wavelengths λ_{max} of the maximum of the main absorption band of polymers **1**−**8** are listed in Table 2. Moreover, for quantitative specification of the refractive index dispersions, we fitted the spectra in the range 600−2000 nm by the Sellmeier equation[73]

$$n^2(\lambda) = 1 + \sum_{i=1}^{2} \frac{a_i \lambda^2}{\lambda^2 - \lambda_i^2} \qquad (2)$$

using two poles. The fit parameters a_1, λ_1, a_2, and λ_2 of the polymers are also given in Table 2. The data of λ_{max} have an estimated uncertainty of ±2 nm because of the broad absorption bands. The experimental error of α_{max} is on the order of 5% and is caused mainly by the experimental error of d. As can be seen in Figure 2a, the MEH-PPV films show a systematic trend to larger values of α_{max} with the increase of M_w. Similarly, the in-plane refractive index n_{TE} increases for higher molecular weight samples, as shown in Figure 2b. This behavior is related to the molecular weight dependence of the average polymer chain orientation in the films as described recently.[35]

Furthermore, Figure 2a and Table 2 show a distinct increase of λ_{max} with M_w of MEH-PPVs **1**−**6**, which indicates an increase in the average effective π-conjugation length L_c.[10] We have observed similar effects in toluene solutions of MEH-PPVs. The number average molecular weights M_n of **1**−**6** vary from 5 to 100 kg/mol, which corresponds to chain lengths between approximately 19 and up to 385 repeat units. The latter number indicates changes of the effective conjugation length far beyond the previously reported saturation limits of another PPV derivative of approximately 30 repeat units[58] or polyenes, which show a saturation limit of 60 repeat units.[52,53] It is an open question currently, whether this is a phenomenon occurring in single chains or whether it is caused by chain aggregation. This deserves further experiments for clarification. We are aware that aggregates can occur already in solution, in particular in the case of high-molecular weight MEH-PPVs.[36−38] We shall discuss the impact of L_c on the THG results of thin films in the next subsection.

THG Spectroscopy. Spectra of the modulus $|\chi^{(3)}|$ of films of polymers **1**, **3**, **4**, **6**, and **8** are shown in Figure 3a, and selected spectra of the corresponding phase angles φ of polymers **1**, **6**, and **8** are presented in Figure 3b. These spectra show the typical three-photon resonance that occurs if the harmonic laser wavelength $\lambda_L/3$ is close to λ_{max}. The maxima of the modulus of $\chi^{(3)}$ are denoted $|\chi^{(3)}_{max}|$ and are displayed in Table 2 together with the harmonic wavelength of this maximum $\lambda_L(\chi^{(3)}_{max})/3$. The three-photon resonance is verified by the phase angle φ_{max}, which is always close to 90° (see Figure 3b and Table 2).

We note that the peaks of the three-photon resonance of $|\chi^{(3)}|$ are always red-shifted as compared to the linear absorption maxima (see Figures 2a and 3a, and Table 2). The harmonic wavelengths $\lambda_L(\chi^{(3)}_{max})/3$ are red-shifted by approximately 5−20 nm versus λ_{max}. This effect is well-known and interpreted by the statistical distribution of effective π-conjugation lengths L_c in a conjugated polymer.[74,75] Because of the super-linear increase of $\chi^{(3)}$ with L_c,[10,11] the longer chain segments with larger L_c dominate the THG response and cause the red-shift of the $|\chi^{(3)}|$ spectrum versus the linear absorption spectrum.

Evaluation of Molecular Weight Effects. The THG spectra shown in Figure 3 reveal a systematic trend to higher values of $|\chi^{(3)}|$ with the increase of M_w at all studied wavelengths. Table

TABLE 2: Linear and Nonlinear Optical Data of Thin Films of MEH-PPVs 1−8[a]

no.	λ_{max} [nm]	α_{max} [10^4 cm^{-1}]	a_1	λ_1 [nm]	a_2	λ_2 [nm]	$\lambda_L(\chi^{(3)}_{max})/3$ [nm]	$\langle\|\chi^{(3)}_{max}\|\rangle$ [10^{-11} esu]	φ_{max} [°]
1	472	13.2	1.418	190	0.145	518.0	480	2.43	92
2	474	13.9	1.402	190	0.137	511.2	480	2.78	89
3	477	15.0	1.431	200	0.165	529.9	490	3.84	91
4	489	16.6	1.416	200	0.208	528.9	510	6.50	88
5	489	18.2	1.550	210	0.164	539.9	510	7.58	93
6	491	18.4	1.564	210	0.188	542.6	510	7.67	84
7	495	19.1	1.573	259	0.190	547.4	510	9.17	97
8	495	19.4	1.583	252	0.197	541.1	510	8.95	92

[a] See text for symbol assignments. The data have the following typical experimental errors: λ_{max}: ± 2 nm; α_{max}: ± 5%; $\lambda_L(\chi^{(3)}_{max})/3$: ± 10 nm; $|\chi^{(3)}_{max}|$: ± 10%; φ_{max}: ± 5°.

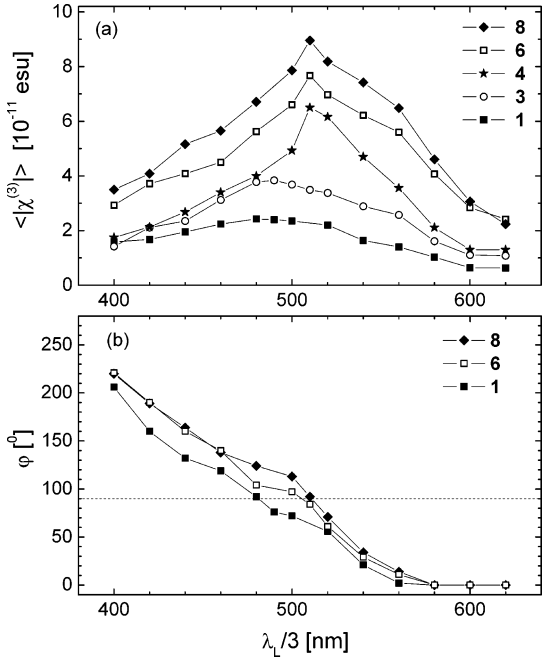

Figure 3. Spectra of the modulus $\langle|\chi^{(3)}|\rangle$ (a) and phase angle φ (b) of the third-order optical susceptibility $\chi^{(3)}(-3\omega,\omega,\omega,\omega)$ measured by THG versus harmonic laser wavelengths $\lambda_L/3$ for thin films of MEH-PPVs **1**, **3**, **4**, **6**, and **8**.

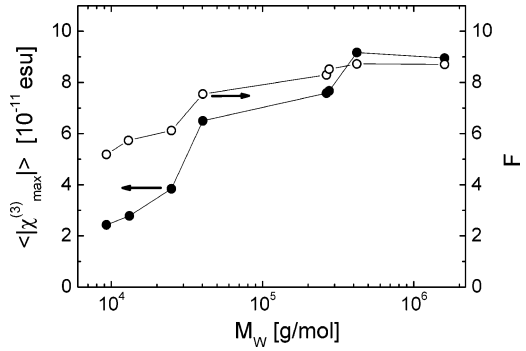

Figure 4. Modulus of the third-order susceptibility $\langle|\chi^{(3)}_{max}|\rangle$ (full circles, left scale) and the total local field factor F (open circles, right scale) of thin films of MEH-PPVs versus their molecular weight (on logarithmic scale).

2 shows that the maxima $|\chi^{(3)}_{max}|$ increase strongly from MEH-PPVs **1**−**8**. This trend is displayed in Figure 4 for comparison, which shows saturation of $|\chi^{(3)}_{max}|$ for the highest molecular weight polymers. We evaluate the impact of M_w on $|\chi^{(3)}_{max}|$ by means of the fundamental relation between the macroscopic $\chi^{(3)}$ and the microscopic molecular hyperpolarizability γ per repeat unit, which is given in the case of THG generation by[10,11,68]

$$\chi^{(3)}(-3\omega,\omega,\omega,\omega) = Nf(3\omega)(f(\omega))^3\gamma(-3\omega,\omega,\omega,\omega) \quad (3)$$

where N is the is the number of repeat units per unit volume, and f is the dimensionless Lorentz local field factor, which is related to the frequency dependent refractive index $n(\omega)$[10,11,68]

$$f(\omega) = (n^2(\omega) + 2)/3 \quad (4)$$

We introduce the total local field factor F

$$F = f(3\omega)[\,f(\omega)]^3 \quad (5)$$

where the fundamental frequency ω refers to the laser wavelength λ_L. We calculate F at the maximum $|\chi^{(3)}_{max}|$ by means of the data of the real parts of the refractive index $n_{TE}(\lambda)$ of thin films for all MEH-PPVs. The data of F are also shown in Figure 4. Although F increases significantly with M_w of the polymer, its change is less than the change of $|\chi^{(3)}_{max}|$. Therefore, we have to discuss two further factors to explain the influence of M_w on $|\chi^{(3)}_{max}|$.

The first factor is related to the molecular hyperpolarizability γ per repeat unit, which is dominated by the tensor component γ_{xxxx} in the direction of the long axis of the one-dimensional conjugated chain segment. The tensor component γ_{xxxx} increases strongly with L_c, as described by the power law $\gamma_{xxxx} \sim L_c^{\mu}$, where the exponent μ is on the order of 4−5.[10] As L_c is also related to λ_{max}, a power law $\chi^{(3)} \sim (\lambda_{max})^{10}$ was derived earlier from a master plot of several conjugated polymers.[10,18] Therefore, we can summarize this and obtain the relation

$$\gamma_{xxxx} \sim (\lambda_{max})^{10} \quad (6)$$

where γ, γ_{xxxx}, L_c, and $\chi^{(3)}$ clearly are ensemble averages that differ for each thin film sample of MEH-PPVs **1**−**8**. As Figure 2 and Table 2 show, λ_{max} increases with M_w. Therefore, we expect that $\chi^{(3)}$ will increase accordingly with λ_{max}.

The second factor that contributes to the increase of $|\chi^{(3)}_{max}|$ with M_w is related to the average orientation of the conjugated chain segments with respect to the layer plane. We have shown recently that the average chain orientation of thin films of MEH-PPV depends strongly on M_w.[34,35] While films made from low-M_w polymers are nearly isotropic, those cast from MEH-PPVs with larger M_w have an increasing amount of PPV chain segments aligned parallel to the layer plane. We performed all THG experiments with incident laser light having TE polarization, i.e., the electrical field vector **E** is parallel to the film plane. Therefore, the angle Θ between **E** and γ_{xxxx} is smaller in the films of higher M_w. As a result, the macroscopic $\chi^{(3)}$ of the films grows with increasing M_w. We treat this effect more quantitatively by writing the in-plane component of the orientation average of $\langle|\chi^{(3)}|\rangle$ of the films, i.e., with **E** parallel to the layer plane in the form

$$\langle|\chi^{(3)}|\rangle = NF\gamma_{xxxx}\langle\cos^4\Theta\rangle \quad (7)$$

following the treatment of Kajzar et al.[62,63] Depending on the arrangements of polymer chains in the film, we can distinguish several situations:[62,63] For a mono-orientation, i.e., all polymer chains are parallel to a given direction, we obtain $\langle\cos^4\Theta\rangle = 1$. The case of two-dimensional disorder, i.e., all polymer chains are parallel to a plane and randomly oriented within this plane, yields $\langle\cos^4\Theta\rangle = 3/8$. The three-dimensional disorder is represented by $\langle\cos^4\Theta\rangle = 1/5$.

For a quantitative description of the molecular weight effects, we investigate now the ratio of the coefficients of eq 7 for the highest and lowest molecular weight MEH-PPVs **8** and **1**, respectively. Using of the data of Table 2, the left side of eq 7 yields the ratio $R_{ls} = \langle|\chi^{(3)}_{max}(\mathbf{8})|\rangle/\langle|\chi^{(3)}_{max}(\mathbf{1})|\rangle = 3.7 \pm 0.8$. The right side of eq 7 gives the following ratios for polymers **8** and **1**: $F(\mathbf{8})/F(\mathbf{1}) = 1.68$ and $\gamma_{xxxx}(\mathbf{8})/\gamma_{xxxx}(\mathbf{1}) = [\lambda_{max}(\mathbf{8})/\lambda_{max}(\mathbf{1})]^{10} = 1.61$. If we attribute the orientation distribution of the chain segments of polymer **8** as two-dimensional, we obtain $\langle\cos^4\Theta(\mathbf{8})\rangle = 3/8$. Similarly, we get $\langle\cos^4\Theta(\mathbf{1})\rangle = 1/5$ if we consider random orientation of polymer **1**. For this limiting case considered here, the ratio of the orientation factors becomes $\langle\cos^4\Theta(\mathbf{8})\rangle/\langle\cos^4\Theta(\mathbf{1})\rangle = 1.88$. Assuming the same density of the films, i.e., $N(\mathbf{8})/N(\mathbf{1}) = 1$, the total ratio of polymers **8**−**1**

of the right side R_{rs} of eq 7 is approximately 5, which is close to the result of the left side $R_{ls} = 3.7 \pm 0.8$. Taking into account that we have probably overestimated the orientation factors by considering the limiting cases only, the agreement of the ratios R_{ls} and R_{rs} of polymers **8** and **1** is rather good. This shows that the observed increase of the third-order nonlinear optical susceptibility with M_w is caused by three main contributions: local field effects, orientation effects, and, presumably, chain ordering effects, which influence the effective conjugation length.

Summary and Conclusions

We used THG spectroscopy to study the third-order nonlinear optical susceptibility $\chi^{(3)}$ of thin spin-coated MEH-PPV films, prepared from polymer samples whose weight-average molecular weight was varied in the broad range of 10−1600 kg/mol. We observed that the $\chi^{(3)}$ values of the films increase as much as a factor of 4 with the molecular weight. This effect is a primary consequence of the preferred in-plane chain orientation in the films of high-M_w polymers as compared to the nearly isotropic chain arrangement in the case of low-M_w polymers. Additionally, we see an increase of λ_{max} at chain lengths between approximately 20 and up to 400 repeat units. This indicates changes of the effective conjugation length, which can also have impact on the $\chi^{(3)}$ values of the films.

A related effect, namely, a M_w dependence of the two-photon absorption coefficient, was observed recently in thin films of poly-3BCMU.[61] Therefore, the molecular weight effect on the nonlinear optical properties is not limited to thin films of MEH-PPV only, but seems to occur more generally and should also be observed for many other conjugated polymers with a rigid backbone. Here we have shown how the molecular weight acts as a key parameter to tailor and control the linear and nonlinear optical constants of thin films of conjugated polymers.

Acknowledgment. We would like to thank Prof. H.-H. Hoerhold for providing us MEH-PPVs **3**, and **4**, and for helpful discussions in the early stage of this work, as well as Covion GmbH for polymer **8**. We also thank G. Herrmann and W. Scholdei for their help with film preparation and optical spectroscopy, respectively. Financial support was given by the German Academic Exchange Services (DAAD, Ph.D. stipend to A.B.), Alexander von Humboldt Foundation (T.A.), Bundesministerium für Bildung und Forschung, and Fonds der Chemischen Industrie (C.B.).

References and Notes

(1) Müllen, K., Wegner, G., Eds. *Electronic Materials: The Oligomer Approach*; Wiley-VCH: Weinheim, Germany, 1998.

(2) Hadziioannou, G., van Hutten, P. F., Eds. *Semiconducting Polymers: Chemistry, Physics and Engineering*; Wiley-VCH: Weinheim, Germany, 2000.

(3) Farchioni, R., Grosso, G., Eds. *Organic Electronic Materials: Conjugated Polymers and Low Molecular Weight Organic Solids*; Springer Series in Materials Science 41; Springer: Berlin, 2001.

(4) Friend, R. H.; Gymer, R. W.; Holmes, A. B.; Burroughes, J. H.; Marks, R. N.; Taliani, C.; Bradley, D. D. C.; Dos Santos, D. A.; Brédas, J. L.; Logdlund, M.; Salaneck, W. R. *Nature* **1999**, *397*, 121−128.

(5) Zaumseil, J.; Friend, R. H.; Sirringhaus, H. *Nat. Mater.* **2006**, *5*, 69−74.

(6) Brabec, C. J.; Sariciftci, N. S.; Hummelen, J. C. *Adv. Funct. Mater.* **2001**, *11*, 15−26.

(7) McGehee, M. D.; Heeger, A. J. *Adv. Mater.* **2000**, *12*, 1655−1668.

(8) Messier, J., Kajzar, F., Prasad, P. N., Ulrich, D., Eds. *Nonlinear Optical Effects in Organic Polymers*; Kluwer: Dordrecht, The Netherlands, 1989.

(9) Kajzar, F., Swalen, J. D., Eds. *Organic Thin Films for Waveguiding Nonlinear Optics*; Gordon and Breach Publishing: Amsterdam, 1996.

(10) Bubeck, C. Nonlinear optical properties of oligomers. In *Electronic Materials: The Oligomer Approach*; Müllen, K., Wegner, G., Eds.; Wiley-VCH: Weinheim, Germany, 1998; Chapter 8, pp 449−478.

(11) Gubler, U.; Bosshard, C. *Adv. Polym. Sci.* **2002**, *158*, 123−191.

(12) Kaino, T.; Kubodera, K.-I.; Tomaru, S.; Kurihara, T.; Saito, S.; Tsutsui, T.; Tokito, S. *Electron. Lett.* **1987**, *23*, 1095−1097.

(13) Bubeck, C.; Kaltbeitzel, A.; Lenz, R. W.; Neher, D.; Stenger-Smith, J. D.; Wegner, G. In *Nonlinear Optical Effects in Organic Polymers*; Messier, J., Kajzar, F., Prasad, P. N., Ulrich, D., Eds.; Kluwer: Dordrecht, The Netherlands, 1989; pp 143−147.

(14) Bradley, D. D. C.; Mori, Y. *Jpn. J. Appl. Phys.* **1989**, *28*, 174−177.

(15) Bubeck, C.; Kaltbeitzel, A.; Grund, A.; LeClerc, M. *Chem. Phys.* **1991**, *154*, 343−348.

(16) Bartuch, U.; Bräuer, A.; Dannberg, P.; Hörhold, H.-H.; Raabe, D. *Int. J. Optoelectron.* **1992**, *7*, 275−279.

(17) Samoc, A.; Samoc, M.; Woodruff, M.; Luther-Davies, B. *Opt. Lett.* **1995**, *20*, 1241−1243.

(18) Mathy, A.; Ueberhofen, K.; Schenk, R.; Gregorius, H.; Garay, R.; Müllen, K.; Bubeck, C. *Phys. Rev. B* **1996**, *53*, 4367−4376.

(19) Gabler, Th.; Waldhäusl, R.; Bräuer, A.; Bartuch, U.; Stockmann, R.; Hörhold, H.-H. *Opt. Commun.* **1997**, *137*, 31−36.

(20) Gabler, Th.; Bräuer, A.; Waldhäusl, R.; Bartuch, U.; Hörhold, H.-H.; Michelotti, F. *Pure Appl. Opt.* **1998**, *7*, 159−168.

(21) Ueberhofen, K.; Deutesfeld, A.; Koynov, K.; Bubeck, C. *J. Opt. Soc. Am. B* **1999**, *16*, 1921−1935.

(22) Samoc, M.; Samoc, A.; Luther-Davies, B.; Bao, Z.; Yu, L.; Hsieh, B.; Scherf, U. *J. Opt. Soc. Am. B* **1998**, *15*, 817−825.

(23) Martin, S. J.; Bradley, D. D. C.; Lane, P. A.; Mellor, H.; Burn, P. L. *Phys. Rev. B* 59, **1999**, 15133−15142.

(24) Bubeck, C.; Ueberhofen, K.; Ziegler, J.; Fitrilawati, F.; Baier, U.; Eichner, H.; Former, C.; Müllen, K.; Pfeiffer, S.; Tillmann, H.; Hörhold, H.-H. *Nonlinear Opt.* **2000**, *25*, 93−104.

(25) Koynov, K.; Goutev, N.; Fitrilawati, F.; Bahtiar, A.; Best, A.; Bubeck, C.; Hörhold, H.-H. *J. Opt. Soc. Am. B* **2002**, *19*, 895−901.

(26) Bader, M. A.; Marowsky, G.; Bahtiar, A.; Koynov, K.; Bubeck, C.; Tillmann, H.; Hörhold, H.-H.; Pereira, S. *J. Opt. Soc. Am. B* **2002**, *19*, 2250−2262.

(27) Fitrilawati, F.; Tjia, M. O.; Pfeiffer, S.; Tillmann, H.; Hörhold, H.-H.; Deutesfeld, A.; Eichner, H.; Bubeck, C. *Opt. Mater.* **2002**, *21*, 511−519.

(28) Schaller, R. D.; Snee, P. T.; Johnson, J. C.; Lee, L. F.; Wilson, K. R.; Haber, L. H.; Saykally, R. J.; Nguyen, T.-Q.; Schwartz, B. J. *J. Chem. Phys.* **2002**, *117*, 6688−6698.

(29) Bahtiar, A.; Koynov, K.; Kibrom, A.; Ahn, T.; Bubeck, C. *Proc. SPIE*, **2006**, *6330*, 63300C-1−63300C-14.

(30) Pfeiffer, S.; Hoerhold, H.-H. *Synth. Met.* **1999**, *101*, 109−110.

(31) Pfeiffer, S.; Hoerhold, H.-H. *Macromol. Chem. Phys.* **1999**, *200*, 1870−1978.

(32) Hörhold, H.-H.; Tillmann, H.; Bader, C.; Klemm, E.; Holzer, W.; Penzkofer, A. *Proc. SPIE* **2002**, *4464*, 317−328.

(33) Holzer, W.; Penzkofer, A.; Tillmann, H.; Hörhold, H.-H. *Synth. Met.* **2004**, *140*, 155−170.

(34) Koynov, K.; Bahtiar, A.; Ahn, T.; Bubeck, C.; Hörhold, H.-H. *Appl. Phys. Lett.* **2004**, *84*, 3792−3794.

(35) Koynov, K.; Bahtiar, A.; Ahn, T.; Cordeiro, R. M.; Hörhold, H.-H.; Bubeck, C. *Macromolecules* **2006**, *39*, 8692−8698.

(36) Nguyen, T.-Q.; Doan, V.; Schwartz, B. J. *J. Chem. Phys.* **1999**, *110*, 4068−4078.

(37) Nguyen, T.-Q.; Martini, I. B.; Liu, J.; Schwartz, B. J. *J. Phys. Chem. B* **2000**, *104*, 237−255.

(38) Schwartz, B. J. *Annu. Rev. Phys. Chem.* **2003**, *54*, 141−172.

(39) Chen, S. H.; Su, A. C.; Huang, Y. F.; Su, C. H.; Peng, G. Y.; Chen, C. A. *Macromolecules* **2002**, *35*, 4229−4232.

(40) Chen, S. H.; Su, A. C.; Chou, H. L.; Peng, K. Y.; Chen, S. A. *Macromolecules* **2004**, *37*, 167−173.

(41) Jeng, U.; Hsu, C.-H.; Sheu, H.-S.; Lee, H.-Y.; Inigo, A. R.; Chiu, H. C.; Fann, W. S.; Chen, S. H.; Su, A. C.; Lin, T.-L.; Peng, K. Y.; Chen, S. A. *Macromolecules* **2005**, *38*, 6566−6574.

(42) Boudrioua, A.; Hobson, P. A.; Matterson, B.; Samuel, I. D. W.; Barnes, W. L. *Synth. Met.* **2000**, *111*−*112*, 545−547.

(43) Wasey, J. A. E.; Safonov, A.; Samuel, I. D. W.; Barnes, W. L. *Opt. Commun.* **2000**, *183*, 109−121.

(44) Tammer, M.; Monkman, A. P. *Adv. Mater.* **2002**, *14*, 210−212.

(45) Gilch, H. G.; Wheelwright, W. L. *J. Polym. Sci., Part A-1: Polym. Chem.* **1966**, *4*, 1337−1349.

(46) Becker, H.; Spreitzer, H.; Ibrom, K.; Kreuder, W. *Macromolecules* **1966**, *32*, 4925−4932.

(47) Becker, H.; Spreitzer, H.; Kreuder, W.; Kluge, E.; Schenk, H.; Parker, I.; Cao, Y. *Adv. Mater.* **2000**, *12*, 42−48.

(48) Ma, H.; Jen, K.-Y.; Dalton, L. R. *Adv. Mater.* **2002**, *14*, 1339−1365.

(49) Stegeman, G. I.; Stolen, R. H. *J. Opt. Soc. Am. B* **1989**, *6*, 652−662.

(50) Stegeman, G. I. *Proc. SPIE* **1993**, *1852*, 75−89.

(51) Slepkov, A. D.; Hegmann, F. A.; Eisler, S.; Elliott, E.; Tykwinski, R. R. *J. Chem. Phys.* **2004**, *120*, 6807−6810.

(52) Samuel, I. D. W.; Ledoux, I.; Dhenaut, C.; Zyss, J.; Fox, H. H.; Schrock, R. R.; Silbey, R. J. *Science*. **1994**, *265*, 1070−1072.

(53) Ledoux, I.; Samuel, I. D. W.; Zyss, J.; Yaliraki, S. N.; Schattenmann, F. J.; Schrock, R. R.; Silbey, R. J. *Chem. Phys.* **1999**, *245*, 1−16.

(54) Gubler, U.; Bosshard, C.; Günter, P.; Balakina, M. Y.; Cornil, J.; Brédas, J. L.; Martin, R. E.; Diederich, F. *Opt. Lett.* **1999**, *24*, 1599−1601.

(55) Martin, R. E.; Gubler, U.; Cornil, J.; Balakina, M.; Boudon, C.; Bosshard, C.; Gisselbrecht, J. P.; Diederich, F.; Günter, P.; Gross, M.; Brédas, J. L. *Chem.—Eur. J.* **2000**, *6*, 3622−3635.

(56) Schulz, M.; Tretiak, S.; Chernyak, V.; Mukamel, S. *J. Am. Chem. Soc.* **2000**, *122*, 452−459.

(57) Meier, H.; Ickenroth, D.; Stalmach, U.; Koynov, K.; Bahtiar, A.; Bubeck, C. *Eur. J. Org. Chem.* **2001**, 4431−4443.

(58) Hsu, J.-H.; Hayashi, M.-T.; Lin, S.-H.; Fann, W.; Rothberg, L. J.; Perng, G.-Y.; Chen, S.-A. *J. Phys. Chem. B* **2002**, *106*, 8582−8586.

(59) Jensen, L.; Astrand, P. O.; Mikkelsen, K. V. *Nano. Lett.* **2003**, *3*, 661−665.

(60) Christensen, R. L.; Faksh, A.; Meyers, J. A.; Samuel, I. D. W.; Wood, P.; Schrock, R. R.; Hultzsch, K. C. *J. Phys. Chem. A* **2004**, *108*, 8229−8236.

(61) Grando, D.; Banfi, G. P.; Fortusini, D.; Ricceri, R.; Sottini, S. *Synth. Met.* **2003**, *139*, 863−865.

(62) Kajzar, F.; Le Moigne, L.; Thierry, A. In *Electronic Properties of Polymers: Orientation and Dimensionality of Conjugated Systems*; Kuzmany, H., Mehring, M., Eds.; Springer Series in Solid State Sciences; Springer-Verlag: Berlin, 1992; pp 202−208.

(63) Rau, I.; Armatys, P.; Chollet, P.-A.; Kajzar, F. *Mol. Cryst. Liq. Cryst.* **2006**, *446*, 23−45.

(64) McBranch, D.; Campbell, I. H.; Smith, D. L.; Ferraris, J. P. *Appl. Phys. Lett*. **1995**, *66*, 1175−1177.

(65) Kranzelbinder, G.; Toussaere, E.; Zyss, J.; Pogantsch, A.; List, E. W. J.; Tillmann, H.; Hörhold, H.-H. *Appl. Phys. Lett.* **2002**, *80*, 716−718.

(66) Losurdo, M.; Giangregorio, M. M.; Capezzuto, P.; Bruno, G.; Babudri, F.; Colangiuli, D.; Farinola, G. M.; Naso, F. *Macromolecules* **2003**, *36*, 4492−4497.

(67) Campoy-Quiles, M.; Etchegoin, P. G.; Bradley, D. D. C. *Phys. Rev. B* **2005**, *72*, 045209-1−045209-16.

(68) Boyd, R. W. *Nonlinear Optics*; Academic Press: Boston, 1992.

(69) Ahn, T.; Ko, S. W.; Lee, J.; Shim, H. K. *Macromolecules* **2002**, *35*, 3495−3505.

(70) Kajzar, F.; Messier, J. *Phys. Rev. A* **1985**, *32*, 2352−2363.

(71) Neher, D.; Wolf, A.; Bubeck, C.; Wegner, G. *Chem. Phys. Lett*. **1989**, *163*, 116−122.

(72) Koynov, K.; Bahtiar, A.; Bubeck, C.; Mühling, B.; Meier, H. *J. Phys. Chem. B* **2005**, *109*, 10184−10188.

(73) Lines, M. E. Physical properties of materials: Theoretical overview. In *Handbook of Infrared Optical Materials*; Klocek, P., Ed.; Marcel Dekker: New York, 1991; p 57.

(74) Kurihara, T.; Mori, Y.; Kaino, T.; Murata, H.; Takada, N.; Tsutsui, T.; Saito, S. *Chem. Phys. Lett.* **1991**, *183*, 534−538.

(75) D'Amore, F.; Zappettini, A.; Facchini, G.; Pietralunga, S. M.; Martinelli, M.; Dell'Erba, C.; Cuniberti, C.; Comoretto, D.; Dellepiane, G. *Synth. Met*. **2002**, *127*, 143−146.